https://doi.org/10.5194/acp-2020-1123
Preprint. Discussion started: 5 November 2020

Atmospheric Chemistry and Physics Discussions

The dynamic-thermal structures of the planetary boundary layer dominated by synoptic circulations and the regular effect on air pollution in Beijing

Yunyan Jiang*[1,2], Jinyuan Xin**[1,2,3], Ying Wang[4], Guiqian Tang[1], Yuxin Zhao[3,5], Danjie Jia[1,2], Dandan Zhao[1,2], Meng Wang[1], Lindong Dai[1], Lili Wang[1], Tianxue Wen[1], Fangkun Wu[1]

[1] State Key Laboratory of Atmospheric Boundary Layer Physics and Atmospheric Chemistry (LAPC), Institute of Atmospheric Physics, Chinese Academy of Sciences, Beijing 100029, China

[2] University of Chinese Academy of Sciences, Beijing 100049, China

[3] Collaborative Innovation Center on Forecast and Evaluation of Meteorological Disasters, Nanjing University of Information Science & Technology, Nanjing, 210044, China

[4] College of Atmospheric Sciences, Lanzhou University, Lanzhou 730000, China

[5] Institude of Atmospheric Composition, Chinese Academy of Meteorological Science, Beijing 100081, China

* These authors contributed equally to this work.

* Correspondence: Jinyuan Xin; email: xjy@mail.iap.ac.cn; phone: (+86)15810006545; address: #40 Huayanli, Chaoyang District, Beijing 100029, China

Abstract. Synoptic circulations play important roles in meteorological conditions and air quality within the planetary boundary layer (PBL). Based on Lamb-Jenkinson weather typing and multiple field measurements, this study reveals the mechanism of how the coupling effects of multiscale circulations influence PBL structure and pollution. Due to the topographic blocking in the daytime, pollutants accumulate in the plain areas horizontally. The sinking divergent flows overlying on the rising convergent flows within the PBL inhibit the continuously upward dispersion of aerosols vertically. At night, the horizontal and vertical coupling mechanisms synergistically worsen the pollution. The large-scale environmental winds and regional-scale breezes affect the pollution directly via the horizontal coupling effect, which generates a pollution convergent zone of different directional flows. The relative strength of flows causes the severely polluted area to move around horizontally from 39°N to 41°N. In addition, the multiscale circulations regulate the mixing and diffusion of pollutants indirectly via the vertical coupling effect, which changes the PBL dynamic-thermal structure. The warm advection transported by the upper environmental winds overlies the cold advection transported by the lower regional breezes, generating strong wind direction shear and advective inversion. The capping inversion and the convergent sinking motion within the PBL suppress massive pollutants below the zero speed zone. The multilayer PBL under cyclonic circulation has no diurnal variation. Weak ambient winds strengthen the mountain breezes observably at night, the temperature inversion can reach 900 m. The nocturnal shallower PBL, consistent with the zero velocity zone between ambient and mountain winds, can reach 600 m. By contrast, the PBL under southwesterly circulation is a mono-layer with obvious diurnal variation, reaching 2000 m in the daytime. The strong winds circulations restrain the development of regional breezes, the zero speed zone is located at 400 m and the inversion is lower than 200 m at night. The PBL under westerly circulation has a hybrid structure with both multiple aerosol layers and diurnal variation. The inversion is generated by the vertical shear of zonal winds. Clean and strong north winds are dominated under anticyclone circulation, the vertical shear and the diurnal variation of thermal field disappear because of strong turbulent mixing, and there is no significant PBL structure. Our results imply that the algorithm of atmospheric environmental capacity under synoptic circulations, such as the cyclonic type, with a multilayer PBL needs to be improved.

https://doi.org/10.5194/acp-2020-1123
Preprint. Discussion started: 5 November 2020

Atmospheric Chemistry and Physics Discussions

Keywords Synoptic Circulation Types, Planetary Boundary Layer, Multiscale Circulations Coupling, Regional Breezes, Air Pollution

1. Introduction

Beijing is the political, economic and cultural center of China. With the recent economic development and acceleration of urbanization, an increasing number of air pollution episodes have emerged and pose a direct threat to human health (Quan et al., 2014; Fu et al., 2014; Cheng et al., 2016; Song et al., 2017). Thus, numerous comprehensive observations and studies on the planetary boundary layer (PBL) and air pollution have been carried out in recent years. Severe pollution is closely related to emissions (Zhang et al. 2012; Wang and Chen 2016), synoptic circulations (Wang et al., 2014; Wu et al., 2017; Liao et al., 2017; Miao et al., 2017a, b), topography (Wang et al., 2018; Zhang et al., 2018) and physical and chemical reaction processes (Sun et al., 2015; Zheng et al., 2015a; Yang et al., 2016). In addition to local emissions in Beijing, massive pollutants are generated in southern Hebei Province and transported northward to Beijing through regional transportation (Miao et al., 2016; Chang et al., 2018; Han et al., 2018). Emissions in a particular area normally do not change much over a short period; however, large-scale atmospheric circulations play a leading role in the transportation, accumulation and dispersion of pollution and thus result in the day-to-day variation of air pollutants (Tai et al. 2012; Zhang 2017; Wang et al., 2018). Zheng et al. (2015b) explored the relationships between AOD and synoptic circulations and found that a uniform surface pressure field in eastern China or a steady straight westerly in the middle troposphere is typically responsible for heavy pollution events. Miao et al. (2017a) specially targeted summertime synoptic types, indicating that the horizontal transport of pollutants induced by the synoptic forcing is the most important factor affecting the air quality of Beijing in summer. They also found that synoptic patterns with high-pressure systems located to the east or southeast of Beijing are the most favorable types for heavy aerosol pollution events. Li et al. (2020) quantitatively analyzed the contributions of different large-scale circulations on PM2.5.

Beijing is located in the North China Plain (NCP) and is surrounded by Yan and Taihang Mountains to the north and west, respectively (Fig. 1b). This semibasin topography blocks and decelerates the relatively weak southerly flows (Li et al., 2007). Aerosol pollutants from southern provinces through regional transportation stagnate and converge in front of the mountains, leading to the accumulation zone of pollution. In addition, Bohai Sea lies to the southeast and is approximately 150 km from Beijing. This unique geographic location and topography results in diurnal variations in the mountain-plain breeze (MPB) and sea-land breeze (SLB) under relative weak synoptic flows. The SLB can penetrate deep into the mainland when it is blooming, and aerosol pollution transported previously over the sea could be recirculated to the Beijing-Tianjin-Hebei region (Liu et al., 2009; Miao et al., 2017a; Bei et al., 2018). As Beijing is surrounded by mountains and relatively far from the Bohai Sea, the intensity of the MPB circulation is much stronger compared to the sea-land breeze circulation in Beijing (Chen et al., 2009; Miao et al., 2015a, b), especially when synoptic circulations dominate in Bohai areas. Miao et al. (2015b) found that the regional-scale MPB circulations can modulate aerosol pollution by lifting or suppressing PBL. Chen et al. (2009) found that the MPB played an important role in the vertical transportation and dispersion of pollutants via the mountain chimney effect.

The PBL structure is also a key factor affecting the distribution and intensity of pollutants in addition to the circulations. The thermal structure of the PBL determines the vertical dispersion of aerosols. In the daytime convective layer, air pollution tends to be mixed vertically and homogeneously because of intensified turbulence and eddies of different sizes by radiation (Stull, 1988). After sunset, the turbulence decays and a stable boundary layer forms with weak turbulence. A radiation inversion on the ground caps the pollutants and leads to the accumulation near the surface. Hu et al. (2014) found that westerly warm advection above the Loess Plateau was

https://doi.org/10.5194/acp-2020-1123
Preprint. Discussion started: 5 November 2020

Atmospheric Chemistry and Physics Discussions

transported over the NCP and imposed a thermal inversion, which acted as a lid and capped the pollution in the boundary layer. The dynamic structure of the PBL, including wind shears and turbulence, can modify air quality by influencing the dispersion and transport processes of air pollutants (Li et al., 2019). Zhang et al. (2020) found that a much weaker vertical wind shear was observed in the lower part of the PBL under polluted conditions, compared with that under clean conditions, which could be caused by the strong ground-level PM2.5 accumulation induced by weak vertical mixing in the PBL. However, due to the lack of comprehensive observation with high vertical resolution, the dynamic and thermal PBL structure, as well as the mechanisms of how the synoptic circulations and regional-scale circulations influence the PBL structure and air quality, is not well understood. Therefore, the relationships among the multiscale circulations, PBL structure and air pollution should be studied in depth. Many classification approaches have been used to discuss the distinctions of different synoptic circulations, which can be mainly divided into subjective and objective methods. Objective weather classification methods have the advantages of convenient operation, high objectivity and efficiency, hence they have been employed widely in recent years (Zhang et al., 2016; Ye et al., 2016; Miao et al., 2017a). In this study, we adopt an objective Lamb-Jenkinson classification scheme to categorize the large-scale atmospheric circulations centered on Beijing. The Lamb-Jenkinson approach has been applied in many previous studies (Huang et al., 2016; Liao et al., 2017; Yu et al., 2017), which have confirmed that the categorization results have clear physical understanding.

This study is based on different synoptic circulations and attempts to investigate the synergetic effects of multiscale circulations on the PBL dynamic-thermal structure and air pollution in detail. The remainder of this paper is organized as follows. Sect. 2 describes the instruments, data and method. Sect. 3 classifies the synoptic circulation types and selects typical types as research objects. Moreover, it further investigates how the coupling mechanism of synoptic circulations and regional-scale circulations changes the dynamic and thermal PBL structure and air pollution. Sect. 4 summarizes the primary conclusions.

2. Data and Method

2.1 Meteorological data

The daily mean sea level pressure (MSLP) and wind fields at 850 hPa were obtained from the National Center for Atmospheric Research (NCAR) reanalysis data (gridded at 2.5˚ × 2.5˚). The divergence and vertical velocity reanalysis data, with a horizontal resolution of 1˚ × 1˚ and a temporal resolution of 1 h, were obtained from Re-analysis Interim (ERA-Interim) of European Centre for Medium-Range Weather Forecasts (ECMWF). The hourly mean wind fields at the surface in the Beijing-Tianjin-Hebei area were collected by hundreds of automatic observation data provided by the China Meteorological Administration (CMA).

2.2 Remote sensing data

The high temporal and spatial resolution data of meteorological fields in the boundary layer are obtained by multiple remote sensing devices. The measuring location of ceilometer, Doppler Lidar and microwave radiometer (MWR) is 39.6°N and 116.2°E, in the courtyard of the Institute of Atmospheric Physics, Chinese Academy of Sciences (Fig. 1b). Steyn et al. (1999) had shown that the aerosol concentration in mixing layer (ML) is close to constant and significantly larger than that in the air above. Thus, the ceilometer (CL51, Vaisala) derives the PBL height by BL-VIEW software according to the minimum value of the local backscatter gradient (Tang et al., 2015). The vertical resolution of the backscatter is 10 meters and the maximal detection range can reach 7.7 km. Three possible PBL heights, with a temporal resolution of 10 minutes, can be output simultaneously to characterize the multiple aerosol layers structure according to the first three largest negative gradients of backscatter. The intensity of backscatter are primarily determined by the concentrations of aerosol particulates; hence, the PBL height derived from the BL-VIEW is a material PBL. A Windcube 100S scanning Doppler Lidar measures the

https://doi.org/10.5194/acp-2020-1123
Preprint. Discussion started: 5 November 2020

Atmospheric Chemistry and Physics Discussions

Doppler shift of aerosol particulate backscatter using the light detection and ranging (Lidar) technique. The vertical measuring range is from 50 m to 3.3 km. Several scanning modes are available and the DBS (Doppler Beam Swinging technique) mode, which includes four LOS (lines of sight) spaced 90° apart with a fixed elevation angle and one vertical LOS, is selected to detect the profiles of winds. The vertical resolution of the profiles is 25 m and the temporal resolution is 20 s. The temperature and relative humidity profiles in RPG-HATPRO MWR are determined by neural network (NN) algorithm, and the vertical resolution of the profiles is 10–30 m in the lowest 0.5 km, 40–90 m from 0.5 km to 2.5 km, 100–200 m from 2 km to 10 km, and the temporal resolution is 1 s.

2.3 Pollutant data

The hourly PM2.5 concentrations in the Beijing-Tianjin-Hebei monitoring sites are acquired from the National Urban Air Quality Real-time Publishing Platform (http://106.37.208.233:20035/) issued by the Ministry of Ecology and Environment. Beijing has 35 air quality monitoring stations and other areas have 68 monitoring sites in total.

2.4 Method

The Lamb-Jenkinson weather typing (LWT) approach is widely adopted in large-scale circulation classification (Lamb 1972; Jenkinson and Collison, 1977) because of its automation and explicit meteorologically meaning. To classify the synoptic circulation types, the daily mean sea level pressures (MSLP) in 2018 and 2019 were used. The LWT scheme is a half-objective categorization method. The weather patterns are predefined and each day can be identified objectively as one certain type according to a small number of empirical rules (Trigo and DaCamara, 2000). As shown in Fig. 1a, 16 gridded pressure data surrounding the study area (Beijing city) were selected to calculate the direction and vorticity of geostrophic wind. The synoptic circulation can be classified into 26 types in total including two vorticity types (cyclonic, C; anticyclonic, A), eight directional types (northeasterly, NE; easterly, E; southeasterly, SE; southerly, S; southwesterly, SW; westerly, W; northwesterly, NW; and northerly, N), and sixteen hybrid types (CN, CNE, CE, CSE, CS, CSW, CW, CNW, AN, ANE, AE, ASE, AS, ASW, AW, and ANW).

The gradient Richardson number (Ri) is the ratio of the buoyancy term to the shear term in the turbulent kinetic equation. It is able to estimate the atmospheric turbulent stability and can be calculated by Eq. 1, where g is the acceleration of gravity and Δz is the height interval between adjacent layers. $\bar{\theta}$ is the mean virtual potential temperature, $\Delta\bar{u}$ and $\Delta\bar{v}$ is the mean zonal and meridional wind speeds within the height interval respectively. Previous studies (Stull, 1988; Guo et al., 2016) suggested that when Ri is smaller than the critical value (0.25), the laminar flow becomes unstable. Thus, we adopt the value of 0.25 as a criterion to determine whether the layer is stable or not.

$$R_i = \frac{\frac{g}{\bar{\theta}}\frac{\Delta\bar{\theta}}{\Delta z}}{(\frac{\Delta\bar{u}}{\Delta z})^2 + (\frac{\Delta\bar{v}}{\Delta z})^2} \quad (1)$$

https://doi.org/10.5194/acp-2020-1123
Preprint. Discussion started: 5 November 2020

Atmospheric Chemistry and Physics Discussions

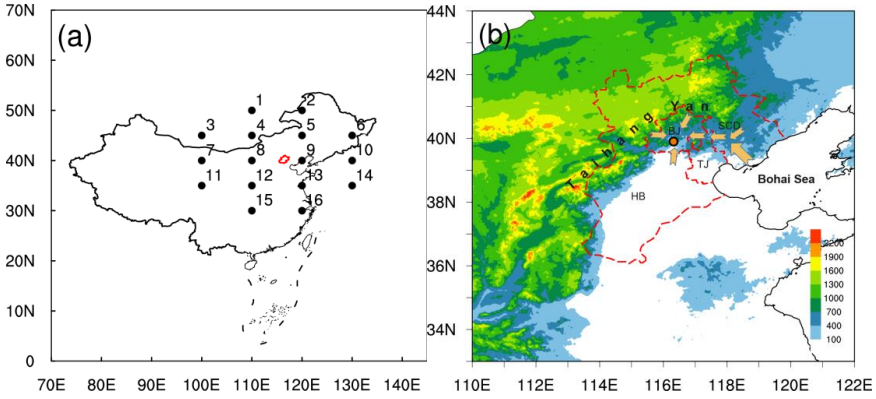

Fig. 1 Location of Beijing city in China (red lines). The 16 black points show the location of the 5°× 10°MSLP grids used for Lamb-Jenkinson weather type classification (a). The terrain height of the North China Plain (shaded, units: m). The filled dots show the locations of remote sensing devices (b). The arrows indicate the horizontal coupling mechanism of how multiscale circulations affect pollution by generating convergent zone.

3. Results and Discussions

3.1 The typical weather types and PM2.5 distribution

Based on the Lamb-Jenkinson weather typing approach, synoptic circulations from 2018 to 2019 were classified into predefined 26 circulation patterns and each day has a specific type. The distributional characteristics of daily averaged PM2.5 concentration, as well as the occurrence frequency of different circulation patterns, were statistically conducted. The occurrence frequencies of the two vorticity and eight directional types were much higher than those of the other sixteen hybrid types, accounting for 75% of total days (Fig. 2). According to the pollution intensity, three pollution types (cyclonic C, southwesterly SW and westerly W) and one clean type (anticyclonic A) occurring most frequently in the NCP were selected as the studied circulation patterns. It was consistent with the results of Li et al. (2020) on the relationship between pollutant concentration and circulation types in northern China. Weather types with high PM2.5 concentration but occurring no more than ten times, such as type CE and type CW, were not discussed in this article. The average and extreme PM2.5 concentrations of type C reached 77 μg/m^3 and 270 μg/m^{3,} respectively, and were much stronger than the other pollution types. Clearly, the cyclonic circulation pattern was more conducive to severe pollution events. The circulation of type A was the most common type, and the PM2.5 concentration was 28 μg/m^3, which was the lowest.

As shown in Fig. 3, the locations of the high and low pressures and the intensity of the wind fields at 925 hPa under different circulation patterns were clearly distinct. In type C, Beijing was located in the center of low pressure, and the sea to the east of China was controlled by an anticyclone (Fig. 3a). Southwesterly winds prevailed, flowing northward to Beijing along the periphery of the anticyclone with an average wind speed of 3 m/s. In type SW, Beijing lay southeast of the low pressure in Mongolia, and the high pressure over the sea was significantly enhanced compared with type C (Fig. 3b). Therefore, southeasterly winds prevailed to the south of Beijing and shifted southwesterly after flowing by. In type W, westerly winds were dominant and converged with southwesterly flows to the north of Beijing (Fig. 3c). The mean velocity of environmental flows in type SW and type W was observably larger than that in type C. In general, the mainland was mainly controlled by low pressure with an anticyclone lying over the sea to the east of China in pollution types C, SW and W, and southerly flows dominated at 925 hPa. By contrast, northern China in the clean type A was occupied by high pressure. Beijing was

https://doi.org/10.5194/acp-2020-1123
Preprint. Discussion started: 5 November 2020

Atmospheric Chemistry and Physics Discussions

located in the center of high pressure with strong northerly winds in the lower level (Fig. 3d).

The pollution intensity is closely related to the large-scale weather circulations. Although the dominant synoptic patterns in different seasons vary greatly, the modulating effects on air pollution of specific circulation types in different seasons are similar (Liao et al., 2017; Li et al., 2020). The spatial distribution of PM2.5 in Beijing under pollution types C, SW, W and clean type A is shown in Fig. 4. Type C had the highest pollution level, with the PM2.5 concentration increasing from 60 μg/m^3 in the northwestern mountainous area to 90 μg/m^3 in the south-central plain area, which was significantly higher than the values for types SW and W. Type A was highly ventilated, with a PM2.5 concentration below 30 μg/m^3 in most areas. Under the influence of semibasin topography surrounded by mountains on three sides (Fig. 1b), the pollution concentrations in all weather types were characterized by a gradual decrease from southeast to northwest in Beijing.

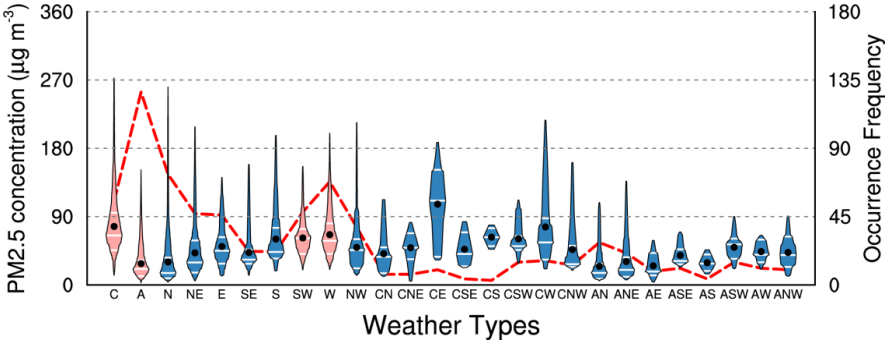

Fig. 2 Daily averaged PM2.5 concentration (box plots, units: 10^{-1} μg m^{-3}) and the occurrence frequencies of 26 weather types (red dashed lines) from 2018 to 2019. The red boxes represent classical types selected for research. The black dots represent the mean values.

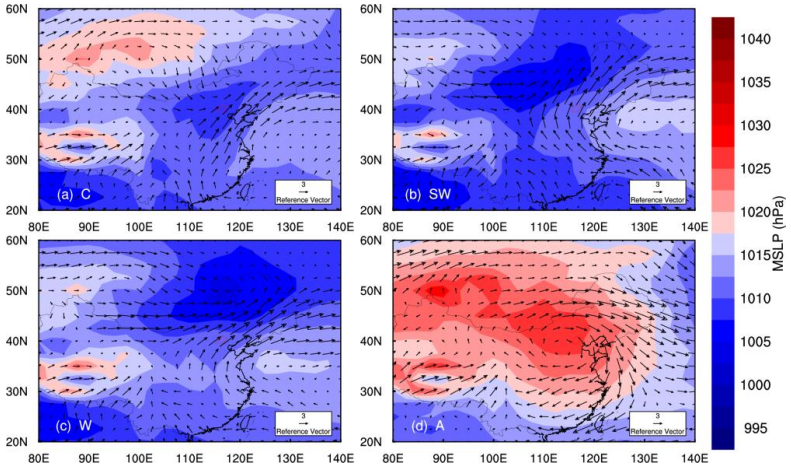

Fig. 3 The daily MSLP (shaded, units: hPa) and wind fields at 925 hPa (vectors, units: m s^{-1}) for types C, SW, W and A from 2018 to 2019.

https://doi.org/10.5194/acp-2020-1123
Preprint. Discussion started: 5 November 2020

Atmospheric Chemistry and Physics Discussions

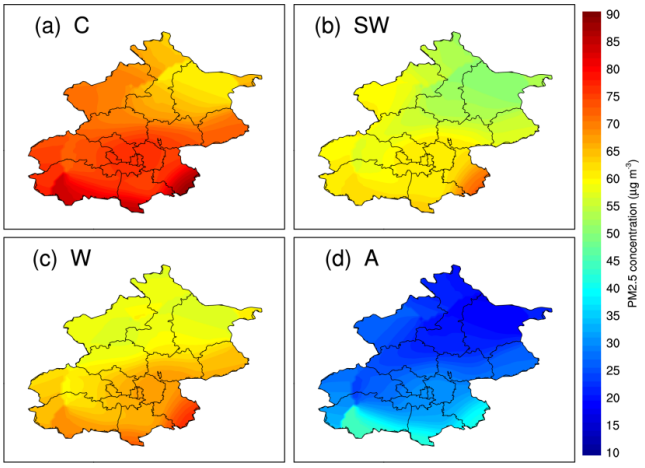

Fig. 4 The averaged PM2.5 concentration (shaded, units: 10^{-1} μg m^{-3}) in Beijing for types C, SW, W and A from 2018 to 2019.

3.2 The flow field and dynamic-thermal structure of the PBL under typical weather types

As mentioned above, due to the special topography and geographical location in Beijing, both large-scale weather circulations and regional-scale thermal circulations have conspicuous effects on modulating pollution. In addition, the thermal and dynamic structure of the PBL also has an appreciable impact on the mixing and diffusion of pollutants. Therefore, the multiscale circulations can not only influence the pollution directly but also influence it by changing the PBL structure indirectly. To reveal the mechanisms of how the coupling effects of multiscale circulations affect the PBL structure and air pollution under different synoptic patterns, we conduct an analysis of the horizontal flow field and vertical PBL structure in depth by choosing typical cases lasting two days in the same weather type (C, SW, W and A).

3.2.1 Multilayer PBL structure under type C circulation

The mainland was governed by low pressure under type C synoptic circulations, and the ambient winds were mainly southwesterly (Fig. 3a). On the afternoon of the 22nd, the plain breezes in central Hebei, which were induced by thermal contrast between the mountain and plain, blocked weak environmental winds and the direct transportation of pollutants to Beijing (Fig. 5a). The westerly and the northerly mountain breezes began to prevail at night while the conversion from sea breeze to land breeze was not obvious (Fig. 5b). The onshore winds in the coastal area were notably larger than the northerly mountain breezes in southern Chengde (SCD), which were diverted to the west and east. The diverted easterly winds converged with the onshore winds, enhancing the easterly winds and the east pollution transport channel. Sun et al. (2019) have found that the pressure gradients between the plain and mountain areas are critical causes of the easterly winds in Beijing. Consequently, easterly winds gathered with mountain breezes and formed a pollution convergent zone. Weak environmental winds not only made the pollution channels hard to establish but also caused the pollutants to recirculate southward by strong downslope breezes further in the early morning (Fig. 5c). A mesoscale convergent belt was generated in southeastern Hebei, providing conditions for the transportation of pollutants later. At noon on the 23rd, the intensified plain winds transported high concentrations of aerosols from the right side of the convergent belt to Beijing (Fig. 5d). Large-scale environmental winds were strengthened and dominated in the afternoon (Fig. 5e), leading to the establishment of the south and east pollution transport channels and further exacerbating the air quality. On the night of the 23rd, easterly winds were observably strengthened again, joining with the downslope

https://doi.org/10.5194/acp-2020-1123
Preprint. Discussion started: 5 November 2020

Atmospheric Chemistry and Physics Discussions

breezes and the ambient southerly flows (Fig. 5f). The four directional airflows formed a convergent zone that caused pollutants to accumulate dramatically in the plain areas. This convergent region that is generated by the coupling effect of large-scale circulation and regional-scale mountain breezes at night also appeared in other pollution types, as will be discussed later.

The PBL under type C circulation presented a multilayer structure without diurnal variation (Fig. 6a). The highly stable structure and weak ambient winds resulted in a higher aerosol concentration near the surface than that in the other pollution types (Fig. 4). The pollution decreased from bottom to top within the PBL and was characterized by a gradient distribution. It is consistent with previous research (Jiang et al., 2020) that the top PBL height is equal to the maximum detection range of wind Lidar. In the daytime, environmental southwesterly winds dominated within the PBL. On the night of the 22nd, meridional winds turned to easterly (Fig. 5b, 6b), and the northerly downslope winds were strengthened simultaneously in the lower PBL (Fig. 5c, 6c). Easterly and northerly winds were up to 600 m so that the directional shear of meridional and zonal winds ascended considerably. The shallower nocturnal PBL coincided with the zero speed zone between the upper environmental winds and lower regional-scale breezes with the largest directional shear (Fig. 6b, c). Variations of the vertical dynamic structure in the PBL drove the thermal structure to adjust. Warm air advected by large-scale southwesterly winds overlay on the cold air advected by regional-scale northeasterly breezes. Consequently, a conspicuous advective temperature inversion occurred from 600 to 900 m (Fig. 6d) accompanied by stable stratification (Fig. 6e). However, the relatively stronger northerly breezes compared to the environmental winds made the pollutants recirculate southward horizontally (Fig. 5c, 6c). Furthermore, the wind shear developed so high that the stable stratification was above 300 m and the inversion was above 600 m; the pollutants dispersed vertically to some extent. Compared to the previous night, the ambient winds on the night of the 23rd were stronger; thus, both south and east transport channels were established, along with the pollution convergent zone (Fig. 5f). The weak easterly and northerly winds were lower than 300 m (Fig. 6b, c), resulting in temperature inversion and stable stratification connected to the ground. A high concentration of pollution was accumulated in the convergent zone horizontally and trapped below the lowest PBL vertically. Thus, the PM2.5 concentration on the night of the 23rd was significantly higher than that on the 22nd.

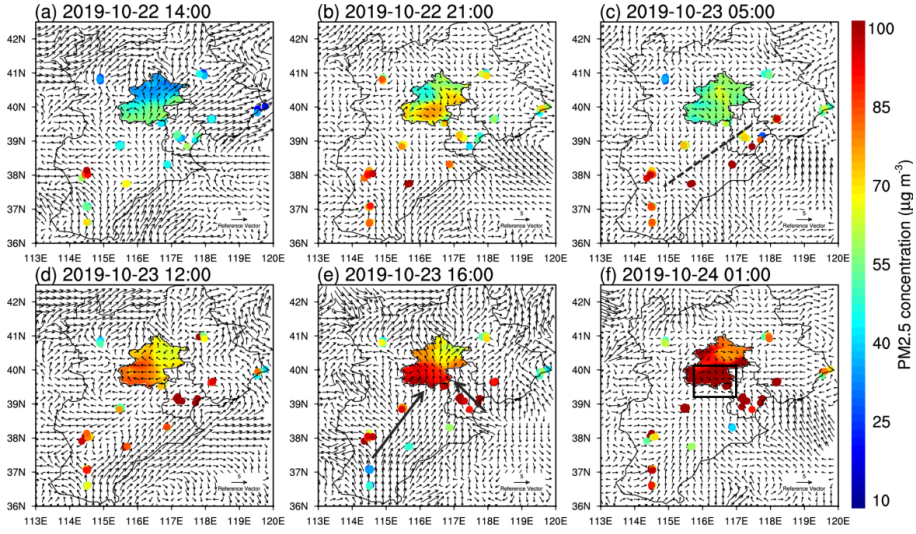

Fig. 5 The surface winds (vectors, units: m s^{-1}) in the NCP and PM2.5 concentration in Beijing (shaded, units: 10^{-1} μg m^{-3}), Hebei and Tianjin (scatter, units: 10^{-1} μg m^{-3}) for type C. The dashed line represents the convergence belt.

https://doi.org/10.5194/acp-2020-1123
Preprint. Discussion started: 5 November 2020

Atmospheric Chemistry and Physics Discussions

The arrow lines represent the pollutant transport channels. The rectangle represents the convergent zone.

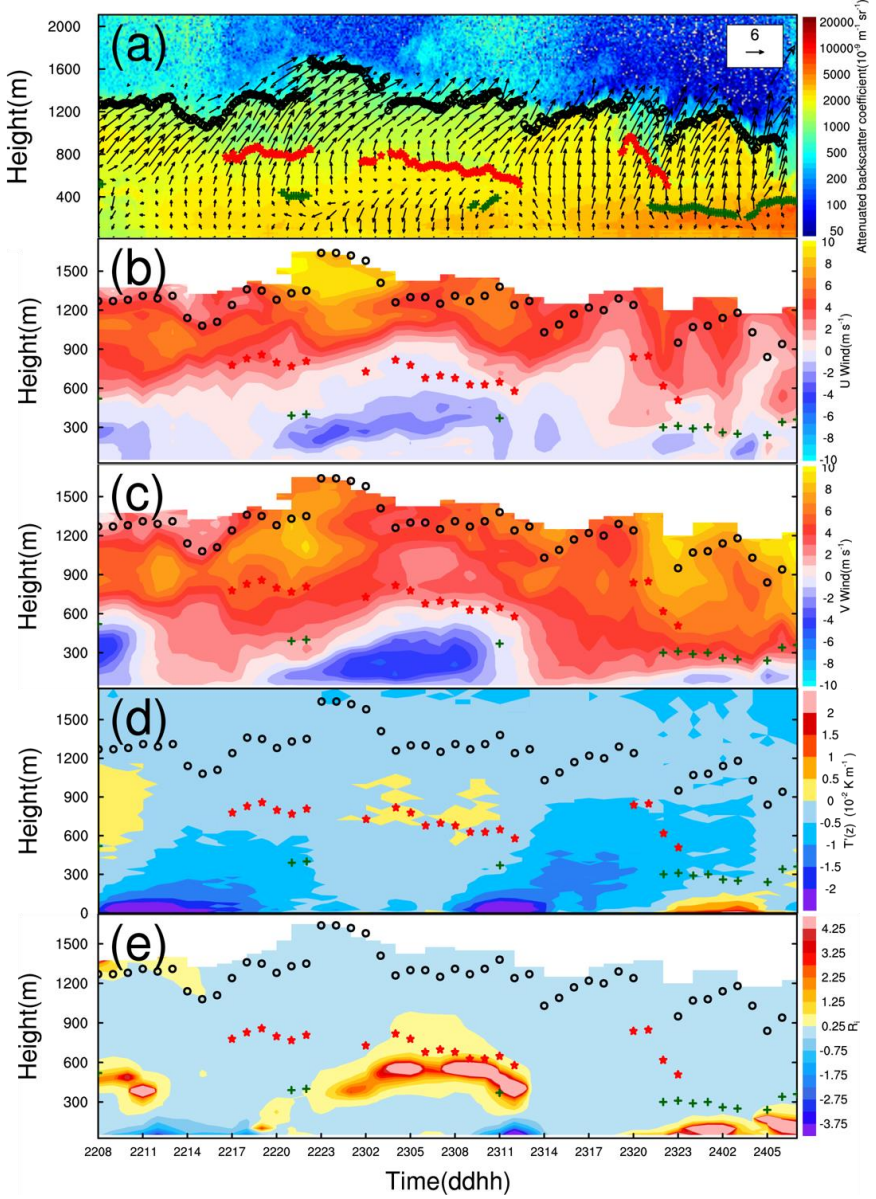

Fig. 6 Attenuated backscatter coefficient (shaded, units: 10^{-9} m^{-1} sr^{-1}) and horizontal winds (vectors, units: m s^{-1}) (a), zonal wind speeds (shaded, units: m s^{-1}) (b), meridional wind speeds (shaded, units: m s^{-1}) (c), gradient of temperature T'(z) (shaded, units: K km^{-1}) (d), and Richardson number (shaded) (e) for type C. The green crosses, red stars and black hollow dots represent the lowest, middle and top PBLH, respectively.

3.2.2 Mono-layer PBL structure under type SW circulation

Under type SW circulation, the easterly wind component increased in southeastern Hebei and the Bohai Sea, and the velocity of environmental winds was appreciably higher than that in type C. (Fig. 3b). On the early

https://doi.org/10.5194/acp-2020-1123
Preprint. Discussion started: 5 November 2020

Atmospheric Chemistry and Physics Discussions

morning of the 26th, mountain breezes carrying clean air masses prevailed in Beijing, and the air quality was good (Fig. 7a). The basic southerly winds dominated in the Beijing-Tianjin-Hebei region in the afternoon, transporting pollutants northward and causing airflow to converge in plain areas (Fig. 7b). However, pollutants were ventilated horizontally by strong ambient winds and diffused vertically by the intensified turbulent mixing within the growing ML, so the aerosol concentration grew slowly during the day (Fig. 8a). At night, the mountain breezes were strengthened while the ambient southerly winds were weakened; hence, the pollutants were transported to Beijing via the east pollution channel (Fig. 7c). Multiscale circulations of different directions joined and generated a convergent zone in the plain area. Afterwards, easterly flows were further strengthened and transported pollutants to Beijing continuously, the severely polluted area moved westward (Fig. 7d, 8a). In the daytime of the 27th, the ambient winds prevailed again, and strong ambient winds removed pollutants by enhancing the ventilation and turbulent mixing (Fig. 7e, 8a). Therefore, the PM2.5 concentration decreased instantly and the air quality in the Beijing-Tianjin-Hebei region improved markedly (Fig. 7f).

Unlike type C, the PBL presented a monolayer structure in type SW, and the aerosol within the PBL was uniformly distributed (Fig. 8a). Furthermore, the PBL had an obvious diurnal variation and the maximum detection distance of wind Lidar was only consistent with the top ML in type SW. The nocturnal PBL and the growing or collapsing ML were usually lower than the maximum detection distance, indicating that there were residual aerosols above the PBL. In the daytime of the 26th, southwesterly winds dominated within the PBL, and the temperature lapse rate was greater than 0.5 °C/100 m. Along with radiation reinforcing turbulent kinetic energy, the PBL rose to 1200 m. Pollutants were transported to Beijing but mixed vertically (Fig. 8a), so the PM2.5 concentration near the surface grew slowly (Fig. 7b). On the night of the 26th, the regional-scale circulation developed upward, and the vertical wind shears between the lower regional breezes and upper environmental winds were strengthened prominently (Fig. 8b, c). The warm advection overlay on the cold advection resulted in advective inversion, forcing the PBL to adjust to become stable, correspondingly (Fig. 8d, e). Similar to type C, a high concentration of pollutants was trapped below the zero wind speed zone where the nocturnal PBL was located. In the daytime of the 27th, large-scale environmental winds within the PBL were strengthened greatly. The PBL height was 800 m higher than that of the previous day; thus, the pollutants were advected horizontally and diffused vertically (Fig. 8a). The basic southerly winds with high speed prevailed in central and southern Beijing on the night of the 27th, preventing the mountain winds from flowing southward (Fig. 7f). As a result, no vertical shear of meridional winds occurred in the dynamic field (Fig. 8c) and no temperature inversion occurred in the thermal field (Fig. 8d). The PM2.5 concentration was further reduced. It can be inferred that the temperature inversion in type SW was generated by the vertical thermal contrast of meridional winds. When the meridional winds were uniformly southerly winds within and above the PBL, the air masses in the upper layer had the same thermal properties as that in the lower layer, which will reduce the vertical wind shear and destroy the stable inversion structure.

https://doi.org/10.5194/acp-2020-1123
Preprint. Discussion started: 5 November 2020

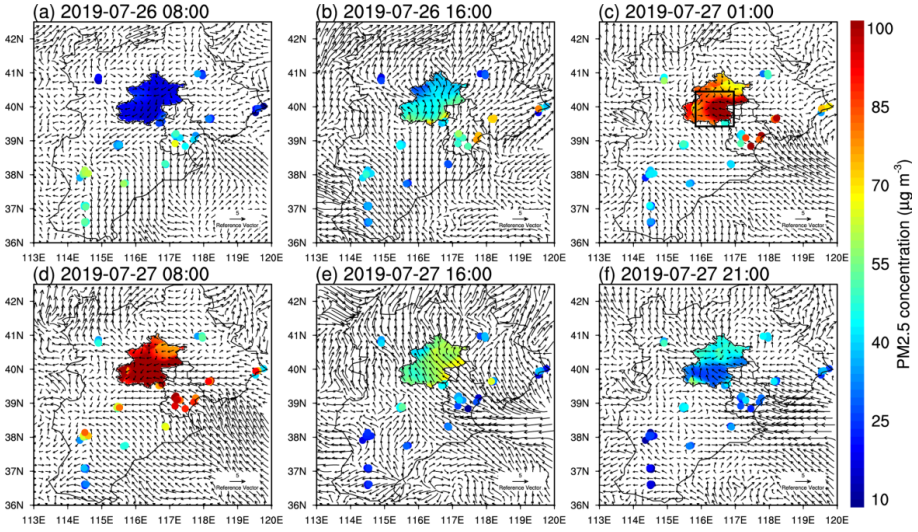

Fig. 7 The surface winds (vectors, units: m s^{-1}) in the NCP and PM2.5 concentration in Beijing (shaded, units: 10^{-1} μg m^{-3}), Hebei and Tianjin (scatter, units: 10^{-1} μg m^{-3}) for type SW. The rectangle represents the convergent zone.

https://doi.org/10.5194/acp-2020-1123
Preprint. Discussion started: 5 November 2020

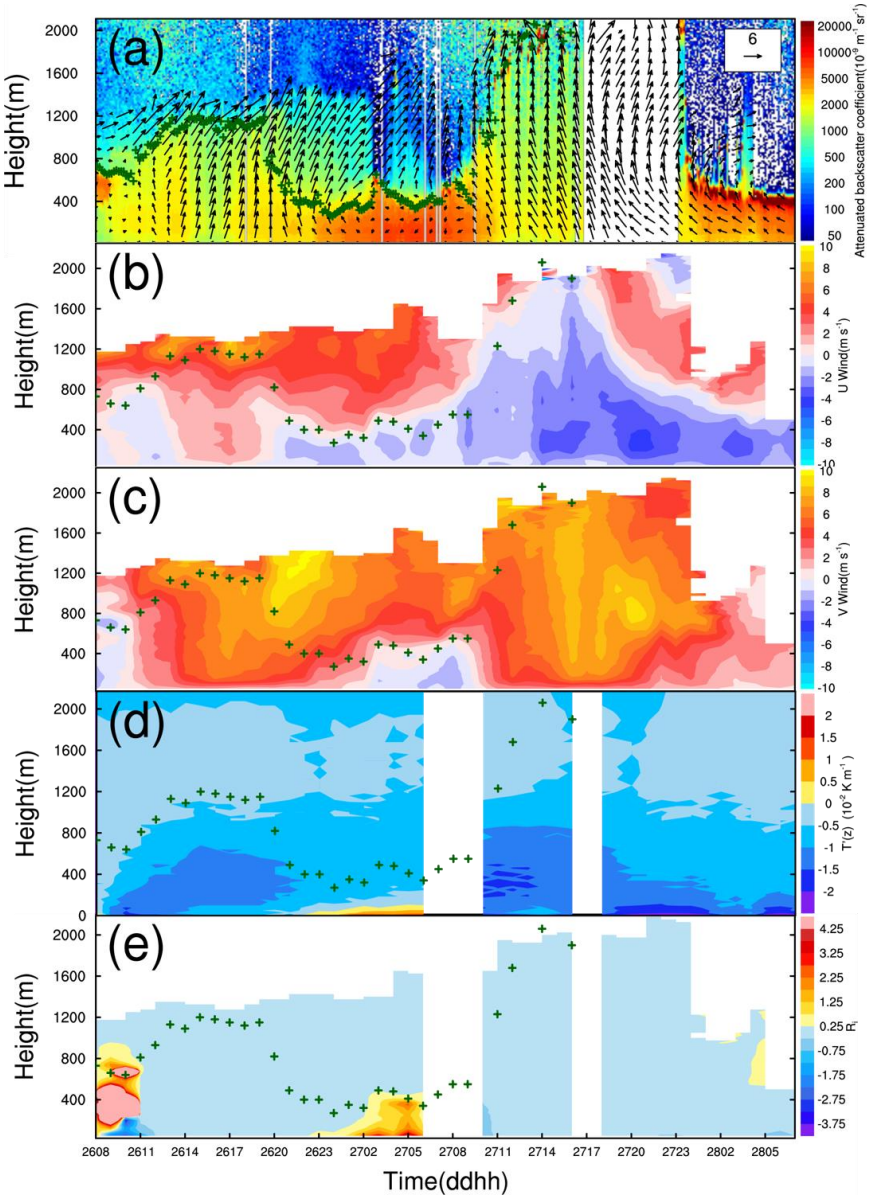

Fig. 8 Attenuated backscatter coefficient (shaded, units: 10^{-9} m^{-1} sr^{-1}) and horizontal winds (vectors, units: m s^{-1}) (a), zonal wind speeds (shaded, units: m s^{-1}) (b), meridional wind speeds (shaded, units: m s^{-1}) (c), gradient of temperature T'(z) (shaded, units: K km^{-1}) (d), and Richardson number (shaded) (e) for type SW. The green crosses represent the PBLH.

3.2.3 Hybrid structure PBL under type W circulation

Under type W circulation, strong easterly winds transported a high concentration of aerosols to Beijing through the east pollution channel, and the PM2.5 concentration had already reached a high level in the early morning (Fig. 9a). Taking the mountain as the boundary, environmental westerly winds prevailed in northwestern

https://doi.org/10.5194/acp-2020-1123
Preprint. Discussion started: 5 November 2020

Atmospheric Chemistry and Physics Discussions

Hebei and southwesterly winds prevailed in southern Hebei in the afternoon. The two directional flows carried pollutants and formed a convergent belt along the western mountains (Fig. 3c, 9b). This distribution of synoptic circulations in type W was conducive to the occurrence of severe pollution around mountains. Similar to other pollution types, the ambient winds converged with region-scale mountain breezes at night, forming a convergent zone (Fig. 9c). The convergent zone moved southward later because of intensified mountain breezes (Fig. 9d). The large velocity of environmental winds leads to strong ventilation (Fig. 9e). In addition, the increasing PBL made the pollutants diluted vertically, and the air pollution was alleviated temporarily. On night of the 16th (Fig. 9f), the synergistic effects of multiscale circulations led to the convergent zone again, and pollution occurred in the easterly flows with a high PM2.5 concentration.

The PBL under type W circulation presented a hybrid structure, having similar characteristics of types C and SW simultaneously. Similar to type C, the aerosol concentration was characterized by a gradient distribution within the multilayer PBL (Fig. 10a). However, the PBL had an obvious diurnal variation, and the maximum detection distance of wind Lidar was only consistent with the top ML in the daytime, similar to type SW. Although the PBL height reached 1600 m in the daytime (Fig. 10a), the PM2.5 concentration at the surface did not decrease observably because of the massive pollution accumulated previously and the continuous emissions and transportation of pollutants (Fig. 9b). The mixing layer collapsed along the zero wind speed of meridional winds after sunset, and the breezes within nocturnal PBL shifted northwesterly at night (Fig. 10b, c). In type W, zonal circulation dominated. The vertical shear of zonal winds was intensified significantly at night, while the vertical shear of meridional winds diminished. Therefore, it can be assumed that the temperature inversion in type W was produced by the vertical shear of zonal winds. The thermal contrast between the upper westerly winds and the lower easterly winds produced a deep inversion layer that existed from the surface to 500 m (Fig. 10d), as well as a stable stratification with a depth exceeding 600 m (Fig. 10e). This is consistent with the findings of Hu et al. (2014) that westerly warm advection from the Loess Plateau was transported over the NCP and imposed a thermal inversion above the PBL. The top of the PBL was consistent with the top of the inversion and zero wind speed zone, and a high concentration of aerosols was trapped below the zero wind speed zone.

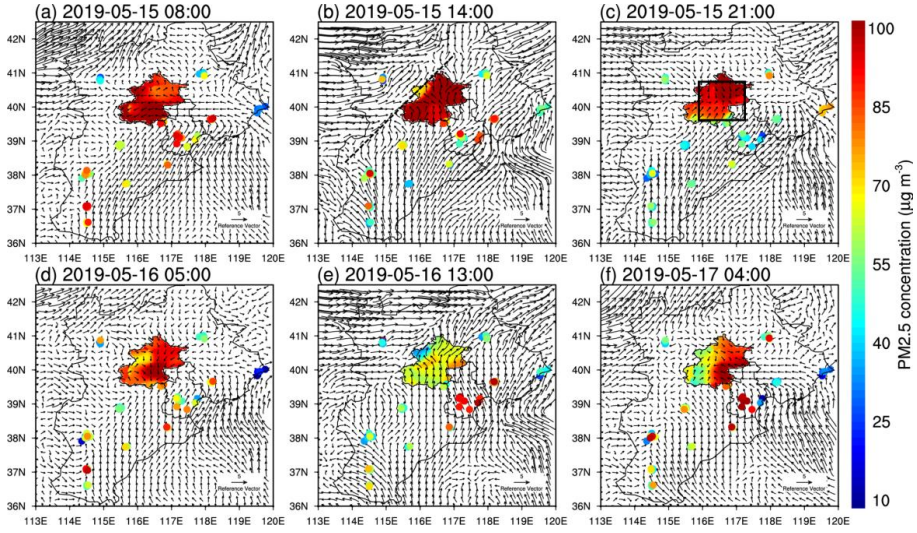

Fig. 9 The surface winds (vectors, units: m s^{-1}) in the NCP and PM2.5 concentration in Beijing (shaded, units: 10^{-1} μg m^{-3}), Hebei and Tianjin (scatter, units: 10^{-1} μg m^{-3}) for type W. The dashed line represents the convergence belt. The rectangle represents the convergent zone.

https://doi.org/10.5194/acp-2020-1123
Preprint. Discussion started: 5 November 2020

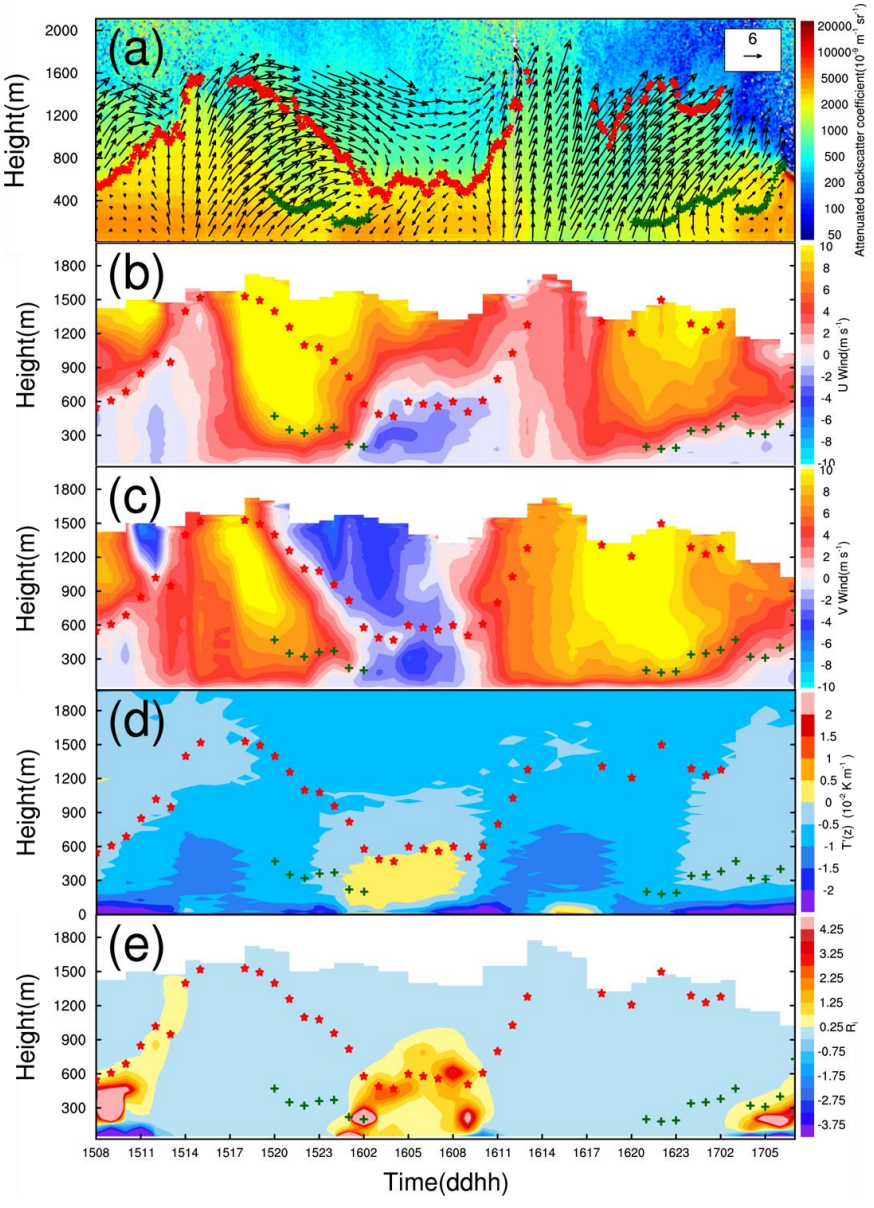

Fig. 10 Attenuated backscatter coefficient (shaded, units: 10^{-9} m^{-1} sr^{-1}) and horizontal winds (vectors, units: m s^{-1}) (a), zonal wind speeds (shaded, units: m s^{-1}) (b), meridional wind speeds (shaded, units: m s^{-1}) (c), gradient of temperature T'(z) (shaded, units: K km^{-1}) (d), and Richardson number (shaded) (e) for type W. The green crosses and red stars represent the low and top PBLH, respectively.

3.2.4 Strong turbulent PBL structure under clean type A circulation

Strikingly different from the circulations of pollution types, the mainland was under high pressure control in the clean type, and northwesterly winds with a high velocity carrying clean air masses moved southward (Fig. 11a). Strong winds were favorable for the turbulent mixing and the vertical dispersion of pollutants. In addition,

https://doi.org/10.5194/acp-2020-1123
Preprint. Discussion started: 5 November 2020

Atmospheric Chemistry and Physics Discussions

the strong ventilation was beneficial to the horizontal spreading of pollutants. Due to the intense turbulent mixing, the vertical wind shear and the diurnal variation of thermal field disappear, and there is no significant PBL structure (Fig. 11a, b). The lapse rate of temperature was greater than 1 °C/100 m, and Ri was less than 0.25 within the PBL (not shown). Although the aerosol concentration of the clean type was far less than that of pollution types, the PBL height was only 500 m at night (Fig. 11a). Sometimes, the PBL in the clean type was even lower than that of pollution types, or extended to 2-3 km swiftly because of the instant upward diffusion of aerosol particulates. Unlike pollution types, the PBL height is inconsistent with the maximum detection range of wind Lidar. Therefore, different circulation types should be distinguished when analyzing the long-term relationships between the PBL height and pollution concentration. As shown in Fig. 12 c and d, under the governing of high pressure, descending and divergent airflows of the clean type dominated the whole lower and middle parts of the troposphere, and the sinking velocity was significantly higher than that of pollution types. The vertical velocity changed little vertically due to the northerly winds with a large speed penetrating downward. The intensity of sinking and divergence was higher at night than that in the day, with the strongest divergence occurring near the surface.

3.3 Multiscale circulations coupling mechanism for air pollution

In addition to horizontal circulations, the vertical motion of basic flows is also a crucial dynamic factor in forming stable stratification during pollution episodes. The pollution types shared similar vertical motion characteristics as shown in Fig. 12. In the daytime, the NCP region was controlled by a rising motion below 900 hPa with a sinking motion overlaying it (Fig. 12a). Correspondingly, the basic flows below 900 hPa presented a convergence, while that above 900 hPa presented a divergence (Fig. 12b). Airflows inside the PBL converged and rose, while the sinking and divergent flows superposed above the PBL, preventing the pollutants from moving upward continuously and making it difficult for the aerosol particulates to diffuse beyond. As a consequence, the pollutants accumulate gradually in the daytime because of the common influences of horizontal topographic blocking and vertical upward mixing with the ML rise. At night, the winds presented a consistent sinking motion below 500 hPa with the largest sinking velocity occurring near the surface (Fig. 12a). Wu et al. (2017) found that the descending motion of synoptic circulations contributed to a reduction in the PBLH by compressing the air mass. In general, the airflow of pollution types is always convergent inside the PBL with the strongest convergence occurring at 950 hPa, regardless of whether it is daytime or nighttime. The height of the nocturnal PBL reduced observably and simultaneously with the convergence zone; meanwhile, divergent downdrafts above the PBL make it difficult for pollutants to diffuse upward (Fig. 12b). Thus, massive pollutants were capped near the surface and accumulated rapidly.

To sum up, different pollution patterns (C, SW and W) have similar influential mechanisms that both horizontal and vertical coupling effects of the multiscale circulations have contributed to air pollution. The horizontal coupling mechanism is shown in Fig. 1b. The environmental winds transport pollutants emitted from southern sources to Beijing, mainly through south and east pollution channels. Large-scale environmental winds and regional-scale breezes are coupled, generating a convergent zone of four directional flows horizontally and aggravating the air pollution directly. The relative strength of winds makes the severely polluted area move around horizontally from 39°N to 41°N. The schematic of Fig. 13 demonstrates that the vertical coupling mechanism further influences the mixing and dispersion of pollution indirectly by changing the PBL structure. In the daytime, the sinking divergent flows overlaying the rising convergent flows within the PBL inhibit the continuous upward dispersion of pollutants. At night, the warm advection transported by the upper environmental winds overlies the cold advection transported by the lower regional breezes, generating strong directional wind shear and advective inversion, which are near the top of regional breezes. This dynamic structure forces the PBL to be a stable stratification. The nocturnal PBL is located at the zero speed zone between the

https://doi.org/10.5194/acp-2020-1123
Preprint. Discussion started: 5 November 2020

Atmospheric Chemistry and Physics Discussions

regional-scale breezes and the environmental winds, and the relative strength of winds determines the PBL height. The capping inversion cooperating with the convergent sinking motion within the PBL suppresses massive pollutants below the zero speed zone.

However, the flow field and the PBL dynamic-thermal structure under different synoptic circulations vary widely with the location and intensity of high and low pressure and wind fields, resulting in differences in pollution. The multilayer PBL under type C circulation has no obvious diurnal variation. Weak ambient winds strengthen the mountain breezes observably at night. Thus, the temperature inversion and zero speed zone can reach 600 m to 900 m vertically, and the pollution convergent zone occurs in the plain areas horizontally. By contrast, the PBL under type SW circulation is a mono-layer with obvious diurnal variation, reaching 2000 m in the daytime. The strong environmental winds restrain the development of regional breezes, the zero speed zone is located at 400 m and the temperature inversion is lower than 200 m at night. The inversion is generated by the vertical shear of meridional winds at night. Southerly winds within and above the PBL having the same thermal properties will diminish the vertical shear and damage the advective inversion structure. The type W circulation is governed by zonal motion and the PBL has a hybrid structure with both multiple aerosol layers and diurnal variations. The vertical comparison of zonal winds leads to a much deeper inversion and stable stratification. The pollution zone under types SW and W circulations is closer to mountainous areas because of strong ambient winds. Furthermore, strong ambient winds make the pollutants ventilate horizontally and diffuse vertically with the growing ML in the daytime.

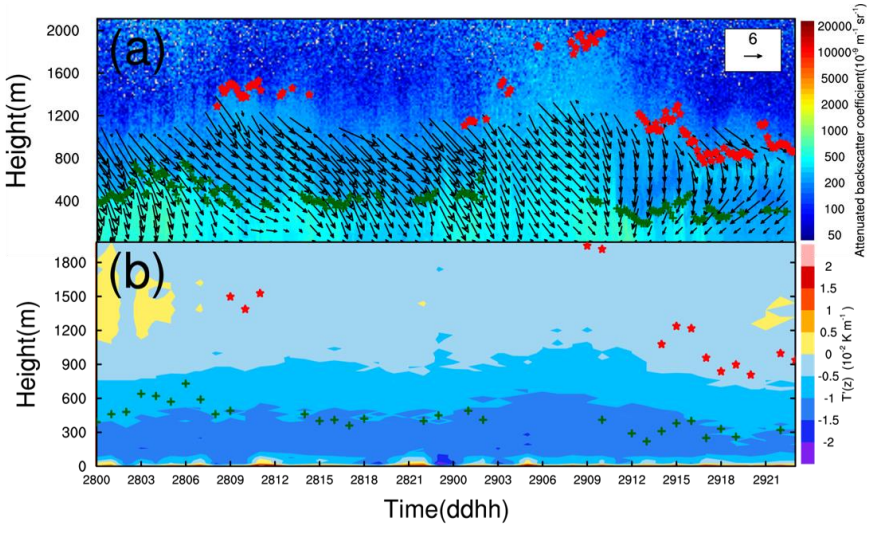

Fig. 11 Attenuated backscatter coefficient (shaded, units: 10^{-9} m^{-1} sr^{-1}) and horizontal winds (vectors, units: m s^{-1}) (a), and gradient of temperature T'(z) (shaded, units: K km^{-1}) (b) for type A. The green crosses and red stars represent the low and top PBLH, respectively.

https://doi.org/10.5194/acp-2020-1123
Preprint. Discussion started: 5 November 2020

Atmospheric Chemistry and Physics Discussions

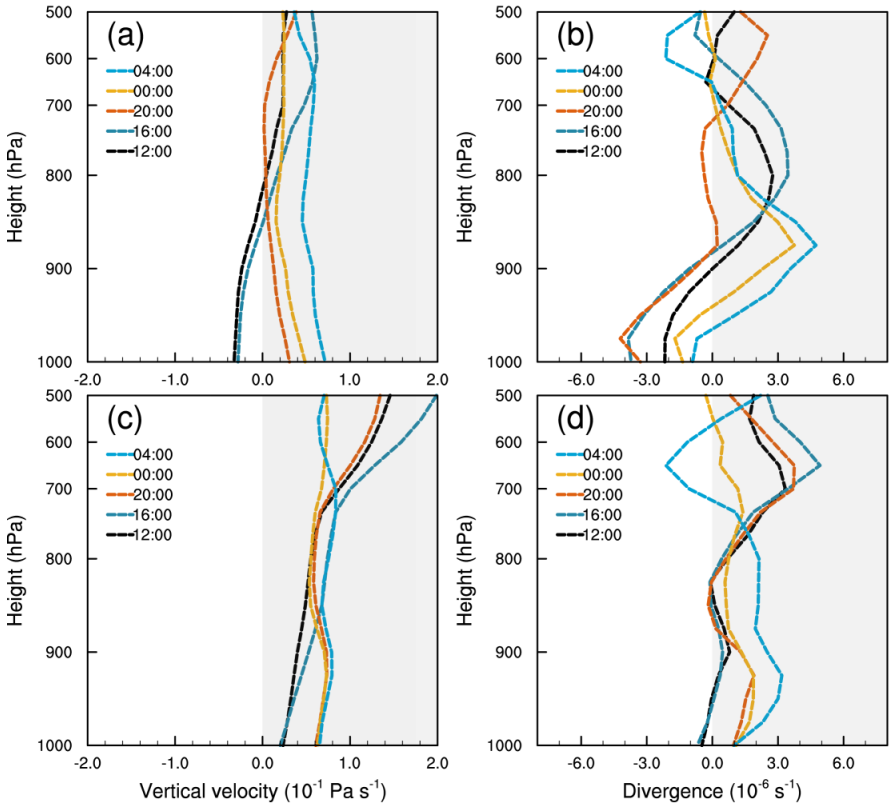

428
429 Fig. 12 The averaged vertical velocity (units: Pa s^{-1}) (a, c) and divergence (units: 10^{-5} s^{-1}) (b, d) of pollution types (a,
430 b) and the clean type (c, d) in the North China Plain

https://doi.org/10.5194/acp-2020-1123
Preprint. Discussion started: 5 November 2020

Atmospheric Chemistry and Physics Discussions

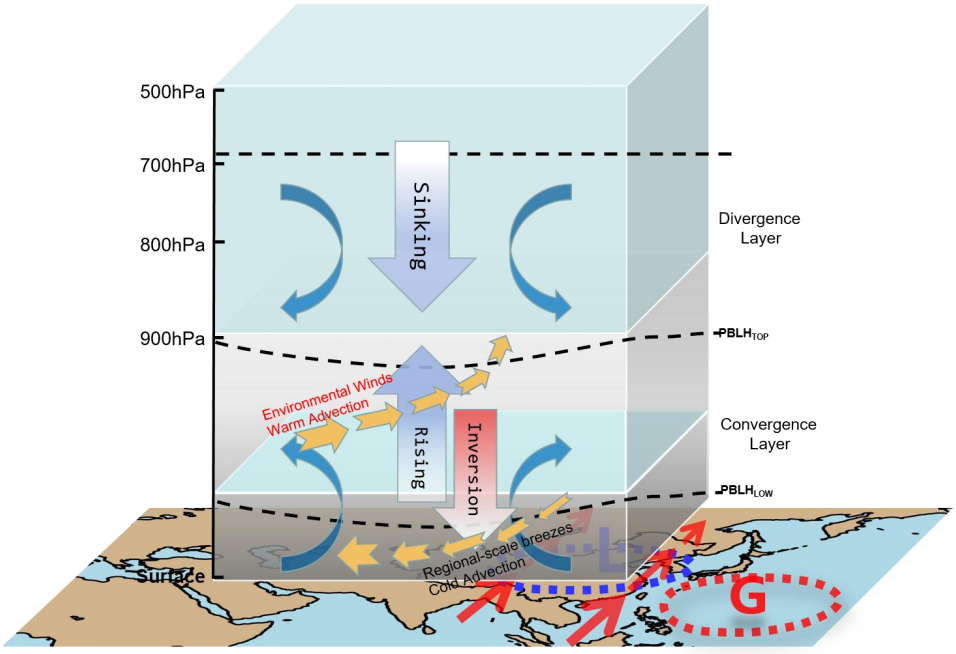

Fig. 13 The vertical coupling mechanism of how multiscale circulations affect pollution by changing the PBL dynamic-thermal structure

4. Conclusions

Based on Lamb-Jenkinson weather typing, the most frequent typical pollution types and clean type were chosen to explore the flow field and the PBL structure under different synoptic patterns. In addition, the horizontal and vertical coupling mechanisms of multiscale circulations, which aggravated pollution synergistically, were further revealed. The results show that different pollution patterns have similar influential mechanisms for air pollution. The large-scale environmental winds and regional-scale breezes, on the one hand, affect the pollution directly via the horizontal coupling effect, which produces a pollution convergent zone. The relative strength of winds makes the severely polluted area move around horizontally. On the other hand, regulate the mixing and diffusion of pollutants indirectly by the vertical coupling effect, which changes the PBL dynamic and thermal structure. Vertical shear between the ambient winds and regional-scale breezes leads to advective inversion and stable stratification, and the relative strength of winds determines the PBL height. Massive pollutants were suppressed below the zero speed zone by the capping inversion and the convergent sinking motion within the PBL. The distinctions of the flow field and PBL dynamic-thermal structure result in the differences of horizontal and vertical pollution, respectively. Based on the fact that both the flow field and PBL structure are dominated by synoptic circulations, the atmospheric environmental capacity (AEC) may vary day by day following the changes in the circulations. Especially when the pollution and meteorological conditions are layered within the PBL, the traditional calculation approach of AEC, which treats the PBL as a uniform and homogenous layer, is no longer applicable. Future work on the quantitative relationships between the PBL structure and air pollution under different weather patterns still needs to be performed. The algorithm of AEC under synoptic circulations with a multilayer PBL, such as cyclonic type circulation, also needs to be improved.

Data availability

https://doi.org/10.5194/acp-2020-1123
Preprint. Discussion started: 5 November 2020

Atmospheric Chemistry and Physics Discussions

The hourly ground level PM2.5 concentration data can be obtained from the National Urban Air Quality Real-time Publishing Platform (http://106.37.208.233:20035/). Other data used in this study can be acquired upon request to the corresponding author.

Competing interests

The authors declare that they have no known competing financial interests or personal relationships that could have appeared to influence the work reported in this paper.

Author contribution

JY performed the idea, methodology, data processing, visualization and writing. XJ provided writing guidance and funding, revised and polished the paper. WY performed supervision. TG contributed to observation data and discussions of results. ZY provided the research data and method. JD, ZD, WM and DL participated in the discussions. WL, WT and WF provided resources. All the authors have made substantial contributions to this article.

Acknowledgments

This study was supported by the Ministry of Science and Technology of China (grant number 2016YFC0202001) and the CAS Strategic Priority Research Program (XDA23020301).

References

Bei, N., Zhao, L., Wu, J., Li, X., Feng, T. and Li, G., 2018. Impacts of sea-land and mountain-valley circulations on the air pollution in Beijing-Tianjin-Hebei (BTH): A case study. Environmental pollution, 234, pp.429-438.

Chang, X., Wang, S., Zhao, B., Cai, S. and Hao, J., 2018. Assessment of inter-city transport of particulate matter in the Beijing-Tianjin-Hebei region. Atmospheric Chemistry & Physics, 18(7).

Chen, Y., Zhao, C., Zhang, Q., Deng, Z., Huang, M. and Ma, X., 2009. Aircraft study of mountain chimney effect of Beijing, China. Journal of Geophysical Research: Atmospheres, 114(D8).

Cheng, Z., Luo, L., Wang, S., Wang, Y., Sharma, S., Shimadera, H., Wang, X., Bressi, M., de Miranda, R.M., Jiang, J. and Zhou, W., 2016. Status and characteristics of ambient PM2. 5 pollution in global megacities. Environment international, 89, pp.212-221.

Fu, G.Q., Xu, W.Y., Yang, R.F., Li, J.B. and Zhao, C.S., 2014. The distribution and trends of fog and haze in the North China Plain over the past 30 years. Atmos. Chem. Phys, 14(21), pp.11949-11958.

Guo, J., Miao, Y., Zhang, Y., Liu, H., Li, Z., Zhang, W., He, J., Lou, M., Yan, Y., Bian, L. and Zhai, P., 2016. The climatology of planetary boundary layer height in China derived from radiosonde and reanalysis data. Atmos. Chem. Phys, 16(20), pp.13309-13319.

Han, S., Liu, J., Hao, T., Zhang, Y., Li, P., Yang, J., Wang, Q., Cai, Z., Yao, Q., Zhang, M. and Wang, X., 2018. Boundary layer structure and scavenging effect during a typical winter haze-fog episode in a core city of BTH region, China. Atmospheric Environment, 179, pp.187-200.

Hu, X.M., Ma, Z., Lin, W., Zhang, H., Hu, J., Wang, Y., Xu, X., Fuentes, J.D. and Xue, M., 2014. Impact of the Loess Plateau on the atmospheric boundary layer structure and air quality in the North China Plain: A case study. Science of the total environment, 499, pp.228-237.

Huang, M., Gao, Z., Miao, S. and Xu, X., 2016. Characteristics of sea breezes over the Jiangsu coastal area, China. International Journal of Climatology, 36(12), pp.3908-3916.

Jenkinson, A.F. and Collison, F.P., 1977. An initial climatology of gales over the North Sea. Synoptic climatology branch memorandum, 62, p.18.

https://doi.org/10.5194/acp-2020-1123
Preprint. Discussion started: 5 November 2020

Atmospheric Chemistry and Physics Discussions

Jiang, Y., Xin, J., Zhao, D., Jia, D., Tang, G., Quan, J., Wang, M. and Dai, L., 2020. Analysis of differences between thermodynamic and material boundary layer structure: Comparison of detection by ceilometer and microwave radiometer. Atmospheric Research, p.105179.

Lamb, H.H. and HH, L., 1972. British Isles weather types and a register of the daily sequence of circulation patterns 1861-1971.

Li, L.J., Ying, W.A.N.G., Zhang, Q., Tong, Y.U., Yue, Z.H.A.O. and Jun, J.I.N., 2007. Spatial distribution of aerosol pollution based on MODIS data over Beijing, China. Journal of Environmental Sciences, 19(8), pp.955-960.

Li, M., Wang, L., Liu, J., Gao, W., Song, T., Sun, Y., Li, L., Li, X., Wang, Y., Liu, L. and Daellenbach, K.R., 2020. Exploring the regional pollution characteristics and meteorological formation mechanism of PM2. 5 in North China during 2013–2017. Environment International, 134, p.105283.

Li, X., Hu, X.M., Ma, Y., Wang, Y., Li, L. and Zhao, Z., 2019. Impact of planetary boundary layer structure on the formation and evolution of air-pollution episodes in Shenyang, Northeast China. Atmospheric Environment, 214, p.116850.

Liao, Z., Gao, M., Sun, J. and Fan, S., 2017. The impact of synoptic circulation on air quality and pollution-related human health in the Yangtze River Delta region. Science of the Total Environment, 607, pp.838-846.

Liu, S., Liu, Z., Li, J., Wang, Y., Ma, Y., Sheng, L., Liu, H., Liang, F., Xin, G. and Wang, J., 2009. Numerical simulation for the coupling effect of local atmospheric circulations over the area of Beijing, Tianjin and Hebei Province. Science in China Series D: Earth Sciences, 52(3), pp.382-392.

Miao, Y., Guo, J., Liu, S., Liu, H., Li, Z., Zhang, W. and Zhai, P., 2017a. Classification of summertime synoptic patterns in Beijing and their associations with boundary layer structure affecting aerosol pollution. Atmos. Chem. Phys, 17(4), pp.3097-3110.

Miao, Y., Guo, J., Liu, S., Liu, H., Zhang, G., Yan, Y. and He, J., 2017b. Relay transport of aerosols to Beijing-Tianjin-Hebei region by multi-scale atmospheric circulations. Atmospheric Environment, 165, pp.35-45.

Miao, Y., Hu, X.M., Liu, S., Qian, T., Xue, M., Zheng, Y. and Wang, S., 2015a. Seasonal variation of local atmospheric circulations and boundary layer structure in the Beijing-Tianjin-Hebei region and implications for air quality. Journal of Advances in Modeling Earth Systems, 7(4), pp.1602-1626.

Miao, Y., Liu, S., Zheng, Y. and Wang, S., 2016. Modeling the feedback between aerosol and boundary layer processes: a case study in Beijing, China. Environmental Science and Pollution Research, 23(4), pp.3342-3357.

Miao, Y., Liu, S., Zheng, Y., Wang, S., Chen, B., Zheng, H. and Zhao, J., 2015b. Numerical study of the effects of local atmospheric circulations on a pollution event over Beijing-Tianjin-Hebei, China. Journal of Environmental Sciences, 30, pp.9-20.

Quan, J., Tie, X., Zhang, Q., Liu, Q., Li, X., Gao, Y. and Zhao, D., 2014. Characteristics of heavy aerosol pollution during the 2012–2013 winter in Beijing, China. Atmospheric Environment, 88, pp.83-89.

Song, C., Wu, L., Xie, Y., He, J., Chen, X., Wang, T., Lin, Y., Jin, T., Wang, A., Liu, Y. and Dai, Q., 2017. Air pollution in China: Status and spatiotemporal variations. Environmental pollution, 227, pp.334-347.

Steyn, D.G., Baldi, M. and Hoff, R.M., 1999. The detection of mixed layer depth and entrainment zone thickness from lidar backscatter profiles. Journal of Atmospheric and Oceanic Technology, 16(7), pp.953-959.

Stull, R. B.: An Introduction to Boundary Layer Meteorology, Kluwer Academic Publishers, Dordrecht, 1988.

Sun, Y., Du, W., Wang, Q., Zhang, Q., Chen, C., Chen, Y., Chen, Z., Fu, P., Wang, Z., Gao, Z. and Worsnop, D.R., 2015. Real-time characterization of aerosol particle composition above the urban canopy in Beijing: insights into the interactions between the atmospheric boundary layer and aerosol chemistry. Environmental science & technology, 49(19), pp.11340-11347.

https://doi.org/10.5194/acp-2020-1123
Preprint. Discussion started: 5 November 2020

Atmospheric Chemistry and Physics Discussions

539 Sun, Z., H. Wang, C. Guo, et al., 2019: Barrier effect of terrain on cold air and return flow of dust air masses, Atmo
540 spheric Research, 220, 81-91.
541 Tai, A.P., Mickley, L.J., Jacob, D.J., Leibensperger, E.M., Zhang, L., Fisher, J.A. and Pye, H.O.T., 2012. Meteorological
542 modes of variability for fine particulate matter (PM 2.5) air quality in the United States: implications for PM
543 2.5 sensitivity to climate change. Atmospheric Chemistry and Physics, 12(6), pp.3131-3145.
544 Tang, G., Zhu, X., Hu, B., Xin, J., Wang, L., Münkel, C., Mao, G. and Wang, Y., 2015. Impact of emission controls on
545 air quality in Beijing during APEC 2014: lidar ceilometer observations. Atmospheric Chemistry & Physics,
546 15(21).
547 Trigo, R.M. and DaCamara, C.C., 2000. Circulation weather types and their influence on the precipitation regime in
548 Portugal. International Journal of Climatology: A Journal of the Royal Meteorological Society, 20(13),
549 pp.1559-1581.
550 Wang, H.J. and Chen, H.P., 2016. Understanding the recent trend of haze pollution in eastern China: roles of
551 climate change. Atmos. Chem. Phys, 16(6), pp.4205-4211.
552 Wang, L., Zhang, N., Liu, Z., Sun, Y., Ji, D. and Wang, Y., 2014. The influence of climate factors, meteorological
553 conditions, and boundary-layer structure on severe haze pollution in the Beijing-Tianjin-Hebei region during
554 January 2013. Advances in Meteorology, 2014.
555 Wang, X., Dickinson, R.E., Su, L., Zhou, C. and Wang, K., 2018. PM2. 5 pollution in China and how it has been
556 exacerbated by terrain and meteorological conditions. Bulletin of the American Meteorological Society, 99(1),
557 pp.105-119.
558 Wu, P., Ding, Y. and Liu, Y., 2017. Atmospheric circulation and dynamic mechanism for persistent haze events in
559 the Beijing–Tianjin–Hebei region. Advances in Atmospheric Sciences, 34(4), pp.429-440.
560 Yang, Y., Liao, H. and Lou, S., 2016. Increase in winter haze over eastern China in recent decades: Roles of
561 variations in meteorological parameters and anthropogenic emissions. Journal of Geophysical Research:
562 Atmospheres, 121(21), pp.13-050.
563 Ye, X., Song, Y., Cai, X. and Zhang, H., 2016. Study on the synoptic flow patterns and boundary layer process of the
564 severe haze events over the North China Plain in January 2013. Atmospheric Environment, 124, pp.129-145.
565 Yu, B., Zhu, B., Dou, J.J., Zhang, W.W., Hu, D.Y., 2017. Classification of air pollution synoptic patterns and air
566 pollutants transport/purification effect by cold front over Hangzhou (in Chinese). China Environ. Sci. 37,
567 452–459.
568 Zhang, Q., He, K. and Huo, H., 2012. Cleaning China's air. Nature, 484(7393), pp.161-162.
569 Zhang, R., 2017. Atmospheric science: Warming boosts air pollution. Nature Climate Change, 7(4), pp.238-239.
570 Zhang, Y., Ding, A., Mao, H., Nie, W., Zhou, D., Liu, L., Huang, X. and Fu, C., 2016. Impact of synoptic weather
571 patterns and inter-decadal climate variability on air quality in the North China Plain during 1980–2013.
572 Atmospheric environment, 124, pp.119-128.
573 Zhang, Y., Guo, J., Yang, Y., Wang, Y. and Yim, S.H., 2020. Vertica Wind Shear Modulates Particulate Matter
574 Pollutions: A Perspective from Radar Wind Profiler Observations in Beijing, China. Remote Sensing, 12(3),
575 p.546.
576 Zhang, Z., Xu, X., Qiao, L., Gong, D., Kim, S.J., Wang, Y. and Mao, R., 2018. Numerical simulations of the effects of
577 regional topography on haze pollution in Beijing. Scientific reports, 8(1), pp.1-11.
578 Zheng, G.J., Duan, F.K., Su, H., Ma, Y.L., Cheng, Y., Zheng, B., Zhang, Q., Huang, T., Kimoto, T., Chang, D. and Pöschl,
579 U., 2015a. Exploring the severe winter haze in Beijing: the impact of synoptic weather, regional transport and
580 heterogeneous reactions. Atmospheric Chemistry and Physics, 15(6), p.2969.
581 Zheng, X.Y., Fu, Y.F., Yang, Y.J. and Liu, G.S., 2015b. Impact of atmospheric circulations on aerosol distributions in
582 autumn over eastern China: observational evidence. Atmospheric Chemistry and Physics, 15(21), p.12115.